

Diagrammatic Approach to Anderson Localization in the Quantum Kicked Rotator

Alexander Altland*

Department of Nuclear Physics, The Weizmann Institute of Science, 76100 Rehovot, Israel

(Received 12 March 1993)

The phenomenon of Anderson localization in the quantum kicked rotator is analyzed by means of concepts which were originally introduced in condensed matter physics. A diagrammatic language similar to the impurity diagram technique employed in the theory of disordered conductors is developed. The method is applied to a calculation of the quantum return probability and leads to results which coincide (apart from numerical factors) with recent numerical findings.

PACS numbers: 05.45.+b, 72.15.Rn

Some years ago it was discovered that the quantum kicked rotator (QKR), traditionally one of the favorite model systems in the theory of quantum chaos, displays a host of phenomena akin to Anderson localization (AL) [1-4]: Unlike its classical counterpart, the dynamics of the *quantum* kicked rotator is not governed by unbound diffusion but rather by an exponential localization of the Hamiltonians' (quasi) eigenstates. Because of surprisingly far-reaching analogies between the phenomenon of localization in the QKR on the one hand and in disordered metals on the other hand, various concepts originally introduced in condensed matter physics are directly applicable to the QKR as well. In particular, it is possible to define QKRs belonging to each of the fundamental symmetry classes (the orthogonal, the unitary, and the symplectic classes) and to realize transitions among them. It has been shown [5] that the localization length characterizing the decay of the wave functions depends in the same universal way on the symmetry as it does in disordered conductors.

All these localization phenomena were discovered numerically. Indeed, the QKR is particularly suitable for numerical studies, since it is by definition a strictly one-dimensional system (which eases its implementation on a computer) while it shares its localization properties with *quasi*-one-dimensional conductors (whose numerical realization is generally much more intricate). To the best of my knowledge, there is no other localizing model system for which numerical data of comparable accuracy are available.

On the other hand, no effective analytical description is available. Fishman, Grempel, and Prange [1] managed to represent the QKR in terms of an Anderson-type tight-binding model. Because of the existence of fairly complex correlations in the corresponding "disorder potential," however, that model turned out to be inconvenient for practical calculations. In this Letter I present a novel analytical approach to the QKR which is comparatively easy to handle and capable of describing the observed localization phenomena. Conceptually, the work may be divided into two parts: First I introduce a diagrammatic representation of the model which is similar to the impurity diagram technique of condensed matter physics. In the second part I make use of existing

knowledge about AL and apply it within the newly developed formalism.

The periodically driven QKR (of orthogonal symmetry; no other symmetry class will be considered in this paper) is defined by the time-dependent Hamiltonian

$$\hat{H}(t) = \frac{1}{2} \hat{l}^2 + k \cos(\hat{\theta}) \sum_n \delta(t - n\tau), \quad (1)$$

where \hat{l} denotes the (angular) momentum operator, $\hat{\theta}$ the (conjugate, $[\hat{l}, \hat{\theta}] = -i$) angle operator, τ the kick time, $k\tau$ the so-called chaoticity parameter, and \hbar is set to unity. Contrary to disordered metals, localization in the QKR takes place in *momentum space*: Consider a particle which is prepared at some initial time $t=0$ in a momentum state $|l\rangle$. Relying on purely classical considerations, one may expect that such a state evolves diffusively in l space on sufficiently large time scales $t \gg \tau$. Indeed, the l -averaged probability $P(\Delta l, t)$ to find the particle after time t in a state $|l+\Delta l\rangle$ obeys the diffusion law [6]

$$P(\Delta l, t) = \frac{2}{(4\pi D_{cl}t)^{1/2}} \exp\left[-\frac{(\Delta l)^2}{4D_{cl}t}\right], \quad (2)$$

with a diffusion constant $D_{cl} = k^2/4$ if the chaoticity parameter exceeds unity [7]. Contrary to the classical rotator, however, this picture breaks down on large time scales $t > k^2\tau$: The wave function does not spread diffusively to infinity but is confined to a region $\Delta l = O(\xi)$ around the initial state where $\xi \sim k^2$ plays the role of a localization length. Both diffusive and localized behavior can be observed in the time dependence of the probability $P(t)$ to return to the initial state after time t . According to Eq. (2) we have for short times $\tau \ll t \ll k^2\tau$, $P(t) = 2/(4\pi D_{cl}t)^{1/2}$ while for large times $t > k^2\tau$, $P(t) \rightarrow \text{const}/\xi$ (the parametric dependence of the asymptotic value follows from probability conservation). In the following, I will introduce a diagrammatic formalism and illustrate its application by an analysis of the return probability. Of course, the method can be used to calculate other observables as well.

The operator governing the time evolution during one elementary step τ reads [4] $\hat{U} = \exp(-i\tau \hat{l}^2/2) \exp[-ik \times \cos(\hat{\theta})] := \hat{P}\hat{J}$. Accordingly the probability to go from state $|l_1 + l\rangle$ to $|l_2 + l\rangle$ in n time steps can be written as

$$W_{l_1+l \rightarrow l_2+l}(n\tau) \equiv |A(l_1+l, l_2+1; n)|^2,$$

where

$$A(l_1+l, l_2+1; n) = \langle l_2+l | (\hat{J}\hat{P})^n | l_1+l \rangle,$$

$$\langle m | \hat{P} | m' \rangle = \exp(-i\tau m^2/2) \delta_{mm'},$$

and $\langle m | \hat{J} | m' \rangle = J_{m-m'}(k)$ is a Bessel function of order $m-m'$. Because of the fact that the \hat{J} depend only on coordinate *differences* the transition amplitudes may alternatively be written as

$$A(l_1+l, l_2+1; n) = \langle l_2 | (\hat{J}\hat{V})^n | l_1 \rangle,$$

with

$$\langle m | \hat{V} | m' \rangle = \exp[-i\tau(m-l)^2/2] \delta_{mm'} := V(m) \delta_{mm'}.$$

These expressions already suggest the analogy to the physics of disordered conductors: The transition from $|l_1\rangle$ to $|l_2\rangle$ consists of free “propagations,” mediated by the Bessel function J (which plays the same role as the

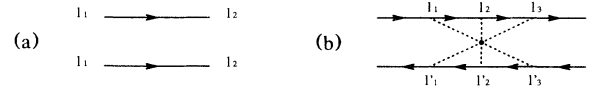


FIG. 1. Basic diagrammatic rules: (a) Propagators. In all figures upper (lower) lines represent propagators $\hat{J} \exp(i\omega_0 + \tau)$ [$\hat{J}^\dagger \exp(-i\omega_0 - \tau)$]. (b) Example of a scattering vertex correlating six coordinates (cf. text).

free Green function in the context of AL), and “scattering” off the momentum diagonal phase factors V [8]. Only the phases contain the averaging coordinate l ; eventually they will play the role of an on-site disorder potential [cf. Eq. (3) below]. As in the impurity perturbation theory of condensed matter physics one may visualize the propagators $J(l-l') := J_{l-l'}(k)[J^\dagger(l-l')]$ by straight lines according to Fig. 1(a). To derive a diagrammatic prescription for the scattering off the phases V , I consider the l average of a typical product of $2n$ factors V as it appears in the calculation of $|A|^2$. It is easily shown that for irrational τ [9]

$$\begin{aligned} \langle V(l_1)V(l_2) \cdots V(l_n)V^*(l'_1)V^*(l'_2) \cdots V^*(l'_n) \rangle &:= \lim_{L_0 \rightarrow \infty} \frac{1}{2L_0+1} \sum_{l=-L_0}^{L_0} [V(l_1) \cdots V^*(l'_n)] \\ &= \begin{cases} \exp[-(i\tau/2)\sum_i(l_i^2 - l_i'^2)], & \sum_i l_i = \sum_i l_i' \\ 0, & \text{otherwise.} \end{cases} \end{aligned} \quad (3)$$

Contrary to the Gaussian distributed disorder potentials which are commonly employed in condensed matter physics, the “potential” of the QKR leads to a correlation of *all* involved coordinates. While a Gaussian correlated potential is formally equivalent to an elastic two-particle interaction [10], the rule Eq. (3) leads to the appearance of m -particle vertices, $m=2,4,\dots,2n$. This is illustrated in Fig. 1(b), where the heavy dot means that the sum of all l coordinates connected to it should equal the sum of all l' coordinates.

As in the context of AL it turns out to be convenient to formulate the theory in the Fourier space of the space where localization takes place. In the present case this implies a transformation from momentum to angle space. Turning additionally from times to frequencies I obtain

$$\begin{aligned} P(l_1-l_2; n) &:= \langle W_{l_1+l \rightarrow l_2+l}(n\tau) \rangle \\ &= \frac{\tau}{2\pi^2} \int d\phi \int d\omega e^{i\phi(l_1-l_2) - i\omega\tau n} \Phi(\phi, \omega), \end{aligned} \quad (4)$$

where

$$\begin{aligned} \Phi(\phi, \omega) &:= \int d\theta d\theta' \Phi(\theta, \theta', \phi, \omega) \\ &:= \int d\theta d\theta' \langle A(\theta_+, \theta'_+; \omega_0+) A^*(\theta_-, \theta'_-; \omega_0-) \rangle, \\ A(\theta, \theta'; \omega) &= \langle \theta | (1 - e^{i\omega\tau} \hat{J}\hat{V})^{-1} | \theta' \rangle, \end{aligned} \quad (5)$$

$$\int d\theta := (1/2\pi) \int_0^{2\pi} d\theta, \quad \theta_{\pm} = \theta \pm \phi/2, \quad \omega_{0\pm} = \omega_0 \pm \omega/2, \quad \omega_0 \in [0, 2\pi]$$

is arbitrary, and the range of the ϕ integra-

tion may be extended over the whole real axis (see below). Equation (4) already anticipates some properties of the l -averaged perturbative expansion of the amplitudes A in powers of V which follow directly from a reformulation of the diagrammatic rules in angle space: First, the l averaging leads to a sort of “angle” conservation in θ space (which is analogous to the momentum conservation of the impurity-mediated interaction in condensed matter physics), whence not four but only three angle integrations appear in Eq. (4). Second, only the energy difference ω between the energy arguments of the transition amplitudes enters the result while ω_0 drops out. Third, the quantity $\Phi(\phi, \omega)$ turns out to be strongly peaked at small values of ϕ and ω whence the upper bound of the ϕ integration is inessential. Finally, the analytic structure of the amplitudes A suggests absorbing the frequency factors $\exp(i\omega\tau)$ in the diagrammatic representation of the propagators, i.e., to extend the definition of the upper (lower) lines in all figures such that they represent the frequency-dependent expressions $\hat{J} \exp(i\omega_0 + \tau)$ [$\hat{J}^\dagger \exp(-i\omega_0 - \tau)$] and not only \hat{J} (\hat{J}^\dagger).

The integral kernel Φ appearing in Eq. (4) is defined in analogy with the density-density response function or polarization propagator in condensed matter physics. Accordingly various concepts of solid state theory may directly be applied to its analysis. Here I have to restrict myself to a brief summary of the main results. Computational details of their derivation will be presented elsewhere [11]. Like in condensed matter physics, so-called

ladder diagrams (cf. Fig. 2) play a particularly important role in the diagrammatic analysis of Φ [12]. More precisely speaking, any diagram containing both crossed and noncrossed scattering lines turns out to be parametrically smaller in powers of $k \gg 1$ than a pure ladder diagram. In this sense, the parameter k plays the same role as the disorder parameter (Fermi momentum \times elastic mean free path) in condensed matter physics. Approximating Φ by a single ladder diagram, one obtains [11] $\Phi(\phi, \omega) \simeq \Phi_0(\phi, \omega) = 1/(\phi^2 D_{cl} - i\omega\tau)$, i.e., the solution of a diffusion equation expressed in Fourier space. Upon insertion into Eq. (4), however, the quantity Φ_0 gives only one half of the right-hand side of Eq. (2). In order to account for the missing factor of 2 one should note that in a time-reversal invariant model *maximally* crossed dia-

grams [cf. the right-hand side of Fig. 3(c)] and ladder diagrams are equivalent [12]. Combining both types one correctly arrives at Eq. (2). On large time scales, however, one expects the onset of localization and the simple diffusive picture needs to be revised. To this end I employ the self-consistent (though not fully rigorous) approach by Vollhardt and Wölfle [13] whose generalization to the present application will be sketched in the following.

To begin with, let me introduce an auxiliary quantity $\tilde{\Phi}(\theta, \theta', \phi, \omega) = J^\dagger(\theta_+) J(\theta_-) e^{-i\omega\tau} \Phi(\theta, \theta', \phi, \omega)$ which differs from Φ just by the trivial truncation of a pair of propagators. In terms of a Dyson equation [cf. the diagrammatic representation in Fig. 3(a)], $\tilde{\Phi}$ may be written as

$$\tilde{\Phi}(\theta, \theta', \phi, \omega) = \tilde{\Phi}_0(\theta, \theta', \phi, \omega) + \int d\theta_1 d\theta_2 \tilde{\Phi}_0(\theta, \theta_1, \phi, \omega) \times J(\theta_{1+}) J^\dagger(\theta_{1-}) e^{i\omega\tau} U(\theta_1, \theta_2, \phi, \omega) J(\theta_{2+}) J^\dagger(\theta_{2-}) e^{i\omega\tau} \tilde{\Phi}(\theta_2, \theta', \phi, \omega), \quad (6)$$

where U is defined as the set of all two-particle irreducible diagrams *without* the single scattering line [cf. Fig. 3(b)]. Before turning to the solution of Eq. (6), let me point out that as a result of fairly general [11,13] considerations, $\tilde{\Phi}(\phi, \omega)$ must behave like $\tilde{\Phi}(\phi=0, \omega) = 1/-i\omega\tau$ as ω approaches 0. For small values of ϕ and ω , any solution of Eq. (6) therefore takes a generalized “diffusive” form

$$\tilde{\Phi}(\phi, \omega) = \frac{1}{D(\omega)\phi^2 - i\omega\tau}, \quad (7)$$

where $D(\omega)$ will in general be frequency dependent. Equation (6) is much too complicated to be exactly solvable. On the other hand, any approximate solution has to result in an expression of the form Eq. (7), i.e., no ϕ - and ω -independent term must appear in the denominator. A particularly efficient way to fulfill this requirement is to employ a certain Ward identity (cf. Ref. [13]) which generalizes to the present context as $\int d\theta U(\theta, \theta', \phi, \omega) = 0$. The derivation of the Ward identity constitutes the most intricate part of this work and will be discussed elsewhere [11]. Coming back to Eq. (6), I notice that it becomes an easily solvable algebraic equation if one makes the (physically plausible) assumption that $\int d\theta \tilde{\Phi}(\theta, \theta', \phi, \omega)$ does not depend on the initial coordinate θ in the long time (small ω) limit. Expanding the propagators attached to U in powers of ϕ and using the Ward identity one thus obtains

$$\tilde{\Phi}(\omega, \phi) = \frac{1}{\tilde{\Phi}_0^{-1} + (k\phi)^2 \int d\theta d\theta' \sin(\theta) U(\theta, \theta', \phi, \omega) \sin(\theta')}, \quad (8)$$

i.e., the problem of finding a solution for $\tilde{\Phi}$ boils down to an analysis of the vertex U . Since we are interested in the behavior of Φ for small ϕ and ω , it is natural to keep only terms which diverge strongest in this limit. A particularly simple infrared divergent contribution to U is the maximally crossed diagram depicted in Fig. 3(c). As a consequence of the model’s time-reversal invariance,

$$[U(\theta, \theta', \phi, \omega)]_{\text{max. crossed}} = \tilde{\Phi}_0(\theta, -\theta', \theta + \theta', \omega),$$

which leads to

$$D(\omega) \simeq D_{cl} - D_{cl}/\pi \int d\phi (D_{cl}\phi^2 - i\omega\tau)^{-1}$$



FIG. 2. Ladder type or diffuson diagram.

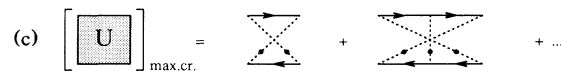
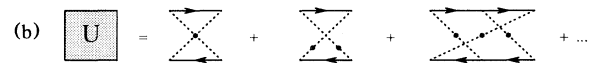


FIG. 3. (a) Dyson equation for the exact kernel $\tilde{\Phi}$. The related quantity Φ may be obtained by attaching a pair of lines to the left-hand side of all blocks. (b) Irreducible vertex U . (c) Contribution of the maximally crossed diagram to U .

upon insertion in Eq. (8). The second term in this equation is the QKR analog of the well-known weak localization correction. This first nonclassical contribution, however, does not yet suffice to explain the strongly localized behavior observed on very small frequency scales. A more general expression for the diffusion constant may be derived by relating the vertex U to the *complete* function Φ (i.e., not just to Φ_0) along the lines of Ref. [13]. As a result one obtains the self-consistent equation

$$D(\omega) = D_{cl} + \frac{D(\omega)}{\pi} \int d\phi \frac{1}{D(\omega)\phi^2 - i\omega\tau}. \quad (9)$$

In the respective limits $\omega > 1/(k^2\tau)$ [$\omega < 1/(k^2\tau)$] corresponding to time scales shorter (longer) than the "localization time" $t_1 \sim \tau k^2$, the equation is solved by $D \approx D_{cl}$ ($D \approx -i\omega\tau k^4/16$). Insertion of the long time expression into Eq. (4) leads to a constant $P(n \gg k^2) \approx 2\pi/k^2$, which overestimates the result of Ref. [4] by a factor of ~ 2 .

Although the fully diagrammatic method presented in this Letter provides a reasonable description of the phenomenon of QKR localization, it suffers from some unsatisfactory aspects and the present state of the theory has to be regarded as incomplete. The approach consists of a manual but self-consistent summation of those diagrams which are expected to be strongest infrared divergent. Because of their rapidly increasing complexity, however, only the simplest of these diagrams (1-loop diagrams in a diagrammatic language) can be kept while more complex but as badly divergent contributions have to be dropped. In QKRs of different symmetries, however, 1-loop diagrams are absent (unitary symmetry) or even have a delocalizing effect (symplectic symmetry) such that higher order diagrams necessarily have to be taken into account. In other words, the present approach is incapable of describing the most interesting transition between

different symmetry classes. I hope, however, that the formulation of the model as it was presented above will provide a suitable basis for the development of a more sophisticated, possibly field theoretical description.

I have profited from discussions with B. L. Altshuler, N. Argaman, F. M. Dittes, S. Fishman, U. Smilansky, and H. A. Weidenmüller and would like to thank MINERVA for financial support.

*Present address: Institut für Theoretische Physik, Zülpicher Strasse 77, 5000 Köln 1, Germany.

- [1] S. Fishman, D. R. Grempel, and R. E. Prange, Phys. Rev. Lett. **49**, 509 (1982); Phys. Rev. A **29**, 1639 (1984).
- [2] D. L. Shepelyansky, Phys. Rev. Lett. **56**, 677 (1986).
- [3] M. Izrailev, Phys. Rep. **196**, 299 (1990).
- [4] T. Dittrich and U. Smilansky, Nonlinearity **4**, 59 (1991).
- [5] R. Blümel and U. Smilansky, Phys. Rev. Lett. **69**, 217 (1992).
- [6] B. V. Chirikov, Phys. Rep. **52**, 263 (1979).
- [7] The extra factor of 2 appearing in the numerator of Eq. (2) is of purely quantum mechanical origin and will be explained below.
- [8] To some extent similar ideas have been formulated within the framework of a semiclassical analysis [N. Argaman, Y. Imry, and U. Smilansky, Phys. Rev. B **47**, 4440 (1993)].
- [9] For rotational values of τ the system does not exhibit localization (cf. Refs. [2,3]).
- [10] A. A. Abrikosov, L. P. Gorkov, and I. E. Dzyaloshinskii, *Methods of Quantum Field Theory in Statistical Physics* (Prentice-Hall, Englewood Cliffs, NJ, 1975).
- [11] A. Altland (to be published).
- [12] A pedagogical discussion of this fact can be found in G. Bergann, Phys. Rep. **T107**, 1 (1984).
- [13] D. Vollhardt and P. Wölfle, Phys. Rev. B **22**, 4666 (1980); *Electronic Phase Transitions*, edited by W. Hanke and Yu. V. Kopaev (Elsevier, Amsterdam, 1992).